Supplementary information for "Drivers of Droplet Formation in East Mediterranean Orographic Clouds"

Romanos Foskinis[1,2,3,4], Ghislain Motos[3], Maria I. Gini[4], Olga Zografou[4], Kunfeng Gao[3], Stergios Vratolis[4], Konstantinos Granakis[4,5], Ville Vakkari[6,7], Kalliopi Violaki[3], Andreas Aktypis[2], Christos Kaltsonoudis[2], Zongbo Shi[8,9], Mika Komppula[10], Spyros N. Pandis[2,11], Konstantinos Eleftheriadis[4], Alexandros Papayannis[1,3], and Athanasios Nenes[2,3*]

[1]Laser Remote Sensing Unit (LRSU), Physics Department, National Technical University of Athens, GR-15780 Zografou, Greece.
[2]Center for Studies of Air Quality and Climate Change, Institute of Chemical Engineering Sciences, Foundation for Research and Technology Hellas, Patras, GR-26504, Greece.
[3]Laboratory of Atmospheric Processes and their Impacts, School of Architecture, Civil & Environmental Engineering, École Polytechnique Fédérale de Lausanne, Lausanne, CH-1015, Switzerland.
[4]ENvironmental Radioactivity & Aerosol Technology for atmospheric & Climate ImpacT Lab, INRASTES, NCSR Demokritos, 15310 Ag. Paraskevi, Attica, Greece.
[5]Climate and Climatic Change Group, Section of Environmental Physics and Meteorology, Department of Physics, National and Kapodistrian University of Athens, Athens, Greece.
[6]Finnish Meteorological Institute, Helsinki, FI-00101, Finland.
[7]Atmospheric Chemistry Research Group, Chemical Resource Beneficiation, North-West University, Potchefstroom, South Africa.
[8]School of Geography, Earth and Environmental Sciences, University of Birmingham, UK.
[9]Key Laboratory of Environmental Optics and Technology, Anhui Institutes of Optics and Fine Mechanics, Chinese Academy of Sciences, Hefei 230031, China
[10]Finnish Meteorological Institute, Kuopio, FI-70211, Finland.
[11]Department of Chemical Engineering, University of Patras, Patras, Greece.

Correspondence to: Athanasios Nenes (athanasios.nenes@epfl.ch) and Alexandros Papayiannis (apdlidar@mail.ntua.gr)

Figure S1 presents the averaged lognormal droplet size distribution for clouds with liquid water content greater than 0.1 g m^{-3}, based on Tables 1 and 2 of Miles et al. (2000) and using the grouping as defined by these authors. It is obvious that any inlet with cut-off size greater than 2.5 μm is may sample cloud droplets when in-cloud.

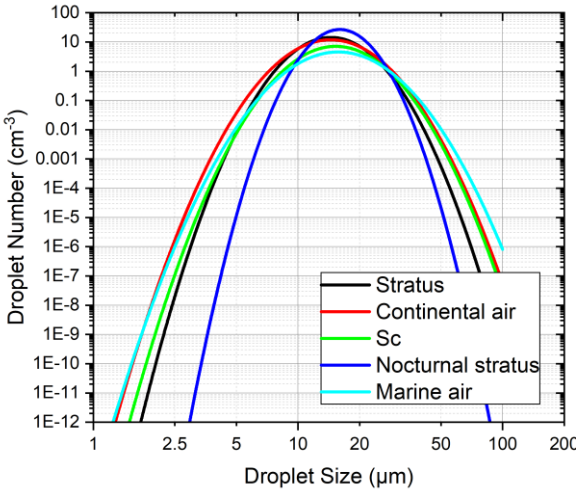

Figure S1. Averaged lognormal droplet size distribution for clouds with liquid water content greater than 0.1 g m^{-3}, based on Tables 1 and 2 of Miles et al. (2000).

Figures S2 (a-e) present the evolution of parameters (σ_w, *eBC*, N_{Total}, SO_4^{2-}) measured at (HAC)², as well as the PBLH, as a function of the horizontal wind velocity and direction. The wind speed is zero at the center of these plots and increases radially up to 14 m s^{-1}. Figure S2f presents the PDF of the wind direction for the cases when (HAC)² is within PBL (red line) or FTL (black line).

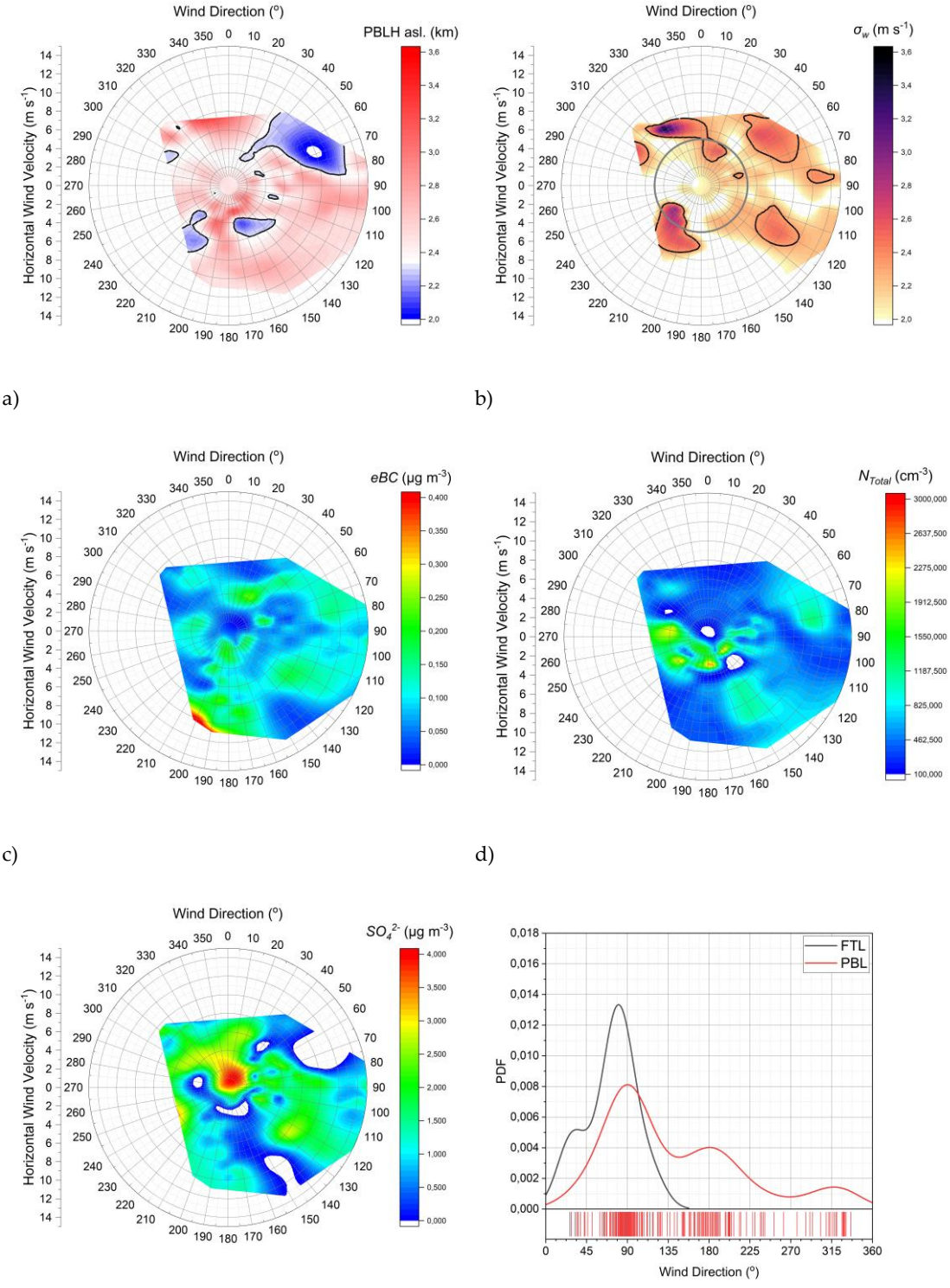

Figure S2 (a-e) Evolution of parameters (σ_w, *eBC*, N_{Total}, SO_4^{2-}) measured at (HAC)² during the whole measuring period, as well as the PBLH, as a function of the horizontal wind velocity and direction. f) The PDF of the wind direction for the cases when (HAC)² is within the PBL (red line) or the FTL (black line).

Figures S3 (a-c) present the statistics of N_{Total}, N_d and D_{eff} measured at $(HAC)^2$ level, when $(HAC)^2$ was within the PBL, or the FTL, under cloud-free or cloudy conditions. We found that the total number of aerosol (N_{Total}) is almost 3 times higher within the PBL, than inside the FTL (Fig. S3b). Additionally, we discuss on the aerosols effects on the droplet formation known as Twomey effect (Twomey, 1977): as shown in Figs. S3(a,b) under cloudy conditions, the increase of the aerosol content (Fig. 3b) within the PBL leads to an increase of N_d (Fig. S3c) resulting to a decrease of the cloud droplet size (Fig. S3c), and thus, enhancing the cloud reflectance (IPCC, 2023)

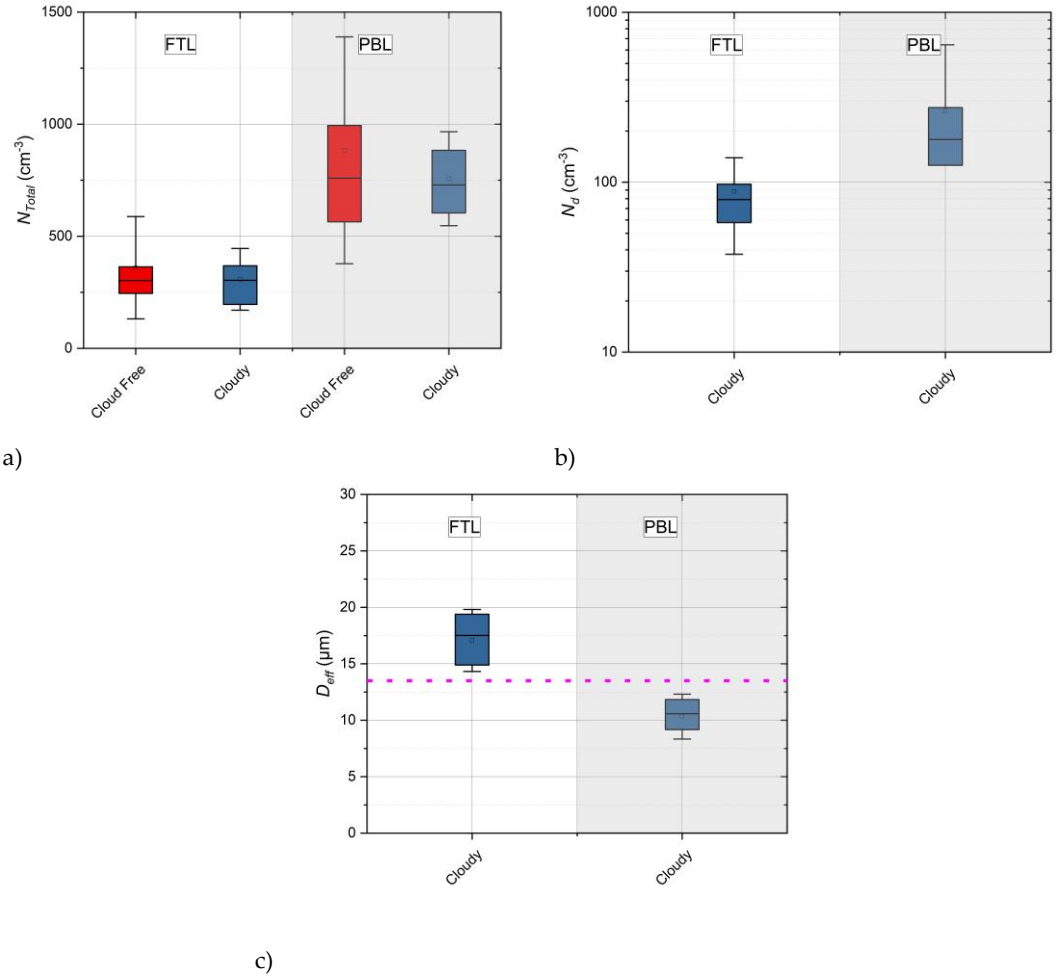

Figure S3. The boxplots of a) N_{Total}, b) N_d and c) D_{eff} measured when $(HAC)^2$ was within the PBL or under cloud-free or cloudy conditions.

The time series of D_{eff} as derived by the PVM-100 are shown in Figure S4 for the cases when $(HAC)^2$ is in the PBL or the FTL. The symbol color represents the *eBC* concentration in μg/m^3 while the shaded area defines the cases dates) when the droplet size was smaller than the characteristic size of the inlet, and so the droplets were able to penetrate the inlet line. Low *eBC* concentrations (blue dots) are observed when $(HAC)^2$ is within the FTL, while high concentrations (white to red) are usually found when $(HAC)^2$ is within the PBL. Furthermore, Figure S4 also shows that clouds within the PBL tend to have more droplets (Figure S3c) with smaller sizes (D_{eff} < 13.5 μm) (cf. Figure S3d), so the droplets with size smaller than 13.5 μm are able to penetrate into the inlet, and that is the reason why the inlet is more sensitive to PBL cloud droplets.

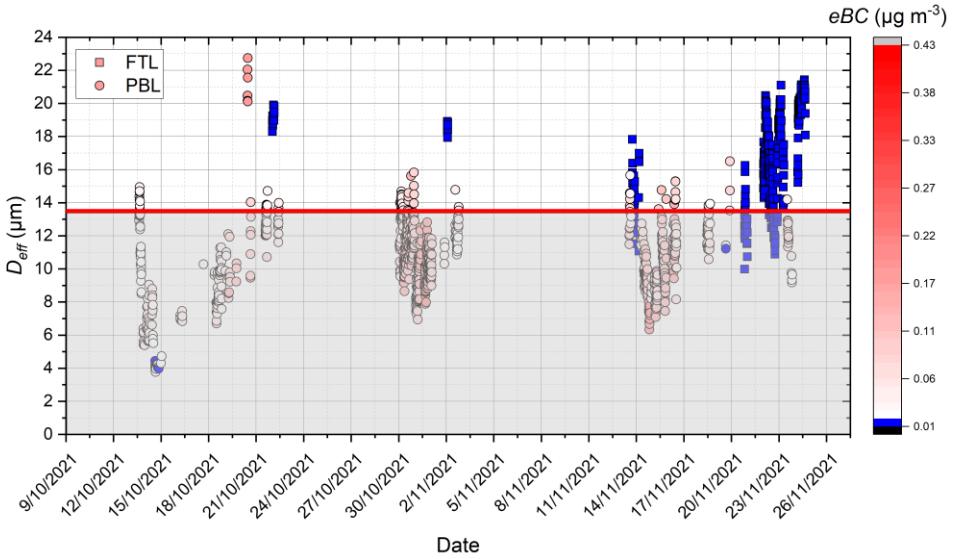

Figure S4. The time series of D_{eff} derived by the PVM-100 when (HAC)2 is within the PBL or the FTL. The symbol color represents the *eBC* concentration in µg/m³ while the shaded area defines the cases dates) when the droplet size was smaller than the characteristic size of the inlet, and so the droplets were able to penetrate the inlet line.

The monthly cloud coverage frequency at (HAC)² was estimated based on continues measurements of RH during the period 1-August-2021 to 1-April-2022, where as a cloud scene is considered, every moment was RH>95%. The results of the monthly cloud coverage frequency at (HAC)² are shown in Figure S5.

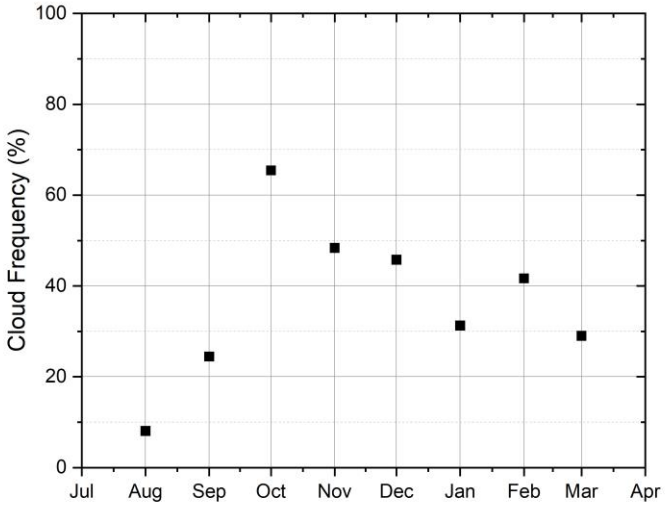

Figure S 5. Cloud frequency at (HAC)² based on continues measurements of RH, where as a cloud scene is considered, every moment was RH>95%.